Polypyrrole/Graphene Composite Films Synthesized via Potentiostatic Deposition

Y. S. Lim,[1] Y. P. Tan,[1,2] H. N. Lim,[1] W. T. Tan,[1] M. A. Mahnaz,[1,3] Z. A. Talib,[4] N. M. Huang,[5] A. Kassim,[6] M. A. Yarmo[7]

[1]Department of Chemistry, Faculty of Science, Universiti Putra Malaysia, 43400 UPM Serdang, Selangor, Malaysia

[2]Centre of Excellence for Catalysis Science and Technology, Universiti Putra Malaysia, 43400 UPM Serdang, Selangor, Malaysia

[3]Laboratory of Biopolymer and Derivatives, Institute of Tropical Forestry and Forest Products (INTROP), Universiti Putra Malaysia, 43400 UPM Serdang, Selangor, Malaysia

[4]Department of Physics, Faculty of Science, Universiti Putra Malaysia, 43400 UPM Serdang, Selangor, Malaysia

[5]Low Dimensional Materials Research Centre, Department of Physics, Faculty of Science, University of Malaya, 50603 Kuala Lumpur, Malaysia

[6]Unit of Chemistry, Faculty of Science, Universiti Sains Islam Malaysia, 71800 Bandar Baru Nilai, Nilai, Negeri Sembilan, Malaysia

[7]School of Chemical Sciences and Food Technology, Faculty of Science and Technology, Universiti Kebangsaan Malaysia, 43650 Bandar Baru Bangi, Selangor, Malaysia

Correspondence to: H. N. Lim (E-mail: janet_limhn@science.upm.edu.my)

ABSTRACT: A one-step electrochemical process has been employed to synthesize composite films of polypyrrole/graphene (PPy/GR) by electrochemical polymerization on indium tin oxide (ITO) from an aqueous solution containing pyrrole monomer, graphene oxide (GO) nanosheets and sodium *p*-toluenesulfonate (NapTS). Thermogravimetric analysis (TGA) confirmed the formation of a composite; the degradation temperature of the new hybrid was between those of PPy and GO. Moreover, the bulbous surface of PPy and the almost transparent tissue-like GO nanosheets were replaced by the new appearance of the composite where the surface was flat but creased. As GO is nonconductive, we deduced that it had been reduced to conducting graphene in the composite film during the electrodeposition process, based on an electrical conductivity study measured with a four-point probe. On average, the electrical conductivity of the PPy/GR composites was twofold higher than that of the pure PPy film, indicating that the incorporation of graphene was able to enhance the conductivity of PPy film. © 2012 Wiley Periodicals, Inc. J. Appl. Polym. Sci. 000: 000–000, 2012

INTRODUCTION

Electronically conducting polymers (ECPs) have attracted much attention because they possess metal-like electrical properties as well as highly desirable polymeric characteristics such as flexibility, low density, and ease of structural modification, leading to an enormous range of potential applications.[1] Of all the ECPs, PPy is popular amongst researchers due to its strong electrical properties, ease of preparation and good environmental stability, which enable its wide application in electronic devices, electrodes for rechargeable batteries and supercapacitors, solid electrolytes for capacitors, sensors and corrosion protection materials.[2–6] Recently, there have been attempts to synthesize polypyrrole composite materials such as polypyrrole-conductive mica, polypyrrole-ferric oxide, polypyrrole-chitosan, and polypyrrole-zinc oxide to achieve a synergistic effect in regards to the properties of the two components.[7–11]

Carbon materials such as carbon black (CB),[12] carbon nanotubes (CNT),[13,14] expanded graphite (EG),[15] and carbon nanofiber (CNF)[5] have been introduced for the preparation of polymer nanocomposites. Even though CNT has been proven to be a conductive filler,[16] the high production cost hinders the utility of CNT to be incorporated into composite materials.[17] Furthermore, metallic catalytic nanoparticles used to prepare CNT still remain as contaminants and dominate the electrochemistry of

CNT even after extensive purification procedures, leading to difficulty in fabricating CNT into reliable sensors and energy storage devices.[18]

A more cost-effective alternative is graphene. Graphene has been introduced for the preparation of polymer nanocomposites to enhance the conductivity of PPy.[19] Graphene is a two-dimensional (2D) one-atom-thick planar sheet of sp^2 bonded carbon atoms arranged in a hexagonal manner, and offers many advantages including a large surface area, excellent conductivity, and high capacity.[20]

Various methods have been employed to synthesize graphene; these include mechanical and chemical exfoliations,[21,22] epitaxial growth via chemical vapor deposition (CVD),[23] unzipping of carbon nanotubes (CNT),[24] and oxidation of graphite followed by reduction.[20] Amongst all the methods, oxidation of graphite is the most popular, owing to its simplicity and scalability. Exfoliation of graphite oxide by sonication gives rise to GO, which is rich in oxygen-containing groups such as epoxy, hydroxyl, ether, and carboxyl randomly distributed on the surface and edges. These functional groups provide a good dispersion stability for GO in polar solution, and facilitate the interaction between GO and a host polymer.[25]

Hybridization of PPy and graphene is believed to be able to generate a new class of nanocomposites with enhanced electrical performance. The most commonly used method for the synthesis of PPy and graphene nanocomposites is *in situ* polymerization.[19,26,27] However, this method requires the use of hydrazine to reduce GO to graphene, which is not only hazardous to the environment and human health,[28] but also compromising on the conductivity of graphene. This is because hydrazine may result in additional chemical groups on graphene sheets, thus increasing the resistance of graphene.[29] Moreover, graphene is poorly dispersible in solvents, causing the 2D nanosheets to agglomerate during the reaction.[30]

Electrochemical polymerization provides a one-step procedure and offers precise control of the thickness of the resulting film.[31] In addition to the speed of polymerization, which can be controlled by the current density,[32] this method also enables mild processing conditions at room temperature,[33] without toxic or excess chemicals,[34] as opposed to other polymerization methods that usually involve multiple steps such as aqueous deposition,[35] *in situ* emulsion,[36] vapor phase polymerization,[37] bulk polymerization,[38] and precipitation.[39]

Recently, Yang et al. prepared PPy/GO composite galvanostatically, and the resulting film was subjected to postelectrochemical reduction to form PPy-reduced GO film.[40] However, pyrrole has been reported to be able to act as a reducing agent to reduce GO to graphene,[30] thus eliminating the need for postelectrochemical step. Previous report shows that galvanostatically deposited PPy film resulted in a thick polymer and was not conductive in comparison to potentiostatically deposited film.[41]

In this study, a simple, fast, green, and one-step electrochemical polymerization of PPy/GR composite films was deposited potentiostatically in the presence of NapTS as a supporting electrolyte. This process allows GO to be reduced to graphene without the need for a prereducing step, which normally involves hazardous chemicals such as hydrazine or postelectrochemical reducing step. Moreover, using GO as the starting material avoids aggregate formation in the reaction solution, resulting in the uniform dispersion of graphene within the network structure of PPy. The effect of the graphene was manifested in the composite films by virtue of the fact their electrical conductivity was increased approximately twofold in comparison to the pure PPy film.

EXPERIMENTAL

Materials

Graphite powder was obtained from Ashbury Graphite Mills, code no. 3061. Sulfuric acid (H_2SO_4, 95–98%), phosphoric acid (H_3PO_4, 85%), potassium permanganate ($KMnO_4$, 99.9%), and hydrogen peroxide (H_2O_2, 30%) were purchased from Systerm. Hydrogen chloride (HCl, 37%) was purchased from Sigma–Aldrich. Pyrrole (99%, Acros organic) was stored at 0°C and distilled prior to use. Sodium *p*-toluenesulfonate (NapTS, 70 %) was purchased from Fluka.

Preparation of GO

GO was synthesized using a simplified Hummer's method.[42] Graphite oxide was obtained by oxidation of 3 g of graphite flakes with $H_2SO_4 : H_3PO_4$ (360 : 40 mL) and 18 g of $KMnO_4$. The mixing process, using a magnetic stirrer, took <5 min to complete. However, to ensure complete oxidation of the graphite, the mixture was stirred for 3 days. During the oxidation, the color of the mixture changed from dark purplish green to dark brown. To stop the oxidation process, H_2O_2 solution was added, whereupon the color of the mixture changed to bright yellow, indicating the high oxidation level of the graphite. The graphite oxide formed was washed with 1 M HCl in aqueous solution, and then repeatedly with deionized water until a pH of 4–5 was achieved. The washing process was carried out using a simple decantation of the supernatant via a centrifugation technique. During the washing process with deionized water, the graphite oxide experienced exfoliation, which resulted in thickening of the GO solution, forming GO gel. The concentration of the GO gel was 4.38 mg mL^{-1}.

Preparation of PPy/GR Composite

PPy/GR composite films were synthesized by electrochemical polymerization from an aqueous solution placed in a one-compartment cell. A potentiostat-galvanostat (Elchema model EQCN-502 Faraday cage) was used for synthesis of the composite films at room temperature. A graphite electrode was used as the counter electrode, while the working electrode was indium tin oxide (ITO)-coated glass. All the potentials were referred to a saturated calomel electrode (SCE). The electrolyte consisted of 0.1–0.5M pyrrole, 1 mg mL^{-1} GO, and 0.1M NapTS. For comparison, a parallel PPy film was synthesized by electrolysis of an aqueous solution containing 0.1–0.5M pyrrole and 0.1M NapTS. The electrochemical deposition was performed at a constant potential of +0.8 V (versus SCE). The electrochemical deposition potential, concentration of GO, and time of polymerization were varied to study their effects on the conductivity of the composite films.
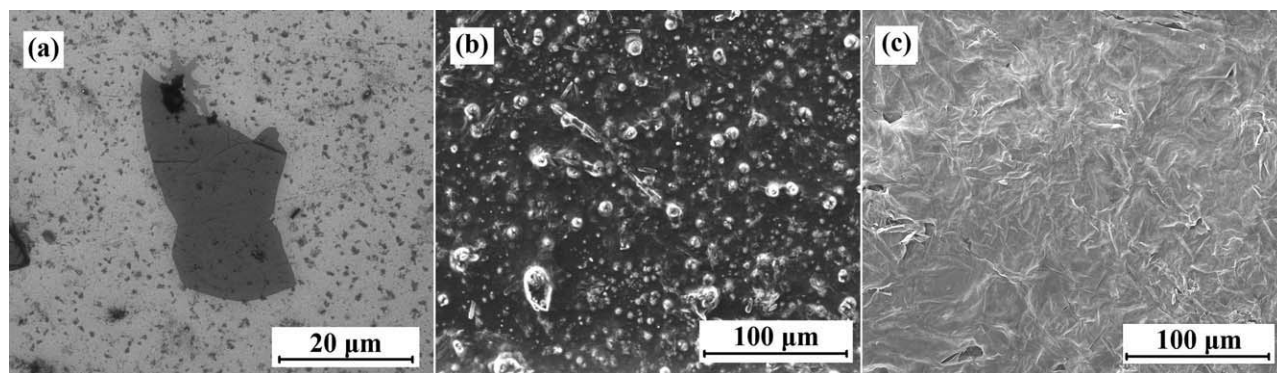
Figure 1. FESEM images of (a) GO, (b) PPy, and (c) PPy/GR, which represent all the composite films. The concentration of PPy used was 0.1*M*.

Characterization

The chemical nature of GO, PPy, and the PPy/GR composite films were analyzed by XPS (Kratos analytical, Axis Ultra^{DLD}). Thermogravimetric analysis was conducted under a nitrogen atmosphere using a TGA Q500 (TA instrument, USA). The resistivity of all the samples was measured using a four-point probe (Jandel Engineering) following the equation:

$$\text{Resistivity} = \frac{\pi}{\ln 2} \times t \times \frac{V}{I} \times R_1$$

$$\text{Conductivity} = \frac{1}{\text{resistivity}}$$

where t is the thickness of the sample, V is the voltage measured, I is the source current, and R_1 is the correction factor for a thin rectangular slice with a value of 0.9822.[43] Field emission scanning electron microscopy images were obtained with a FEI Nova NanoSEM 400 operated at 10.0 kV.

RESULTS AND DISCUSSION

Figure 1 shows SEM images of GO, PPy, and PPy/GR. The GO nanosheets have a thin paper-like appearance, which is translucent [Figure 1(a)]. On the contrary, the PPy film is bulbous; typical of the rough surface of PPy,[44] as depicted in Figure 1(b). Interestingly, the physical appearances of the individual materials changed drastically when they were hybridized into a composite. The prepared composite appeared to have an almost flat surface even though creases could be found on it [Figure 1(c)]. It is evident that a composite, comprising GO and PPy prepared using the electrodeposition process, had been formed, as the morphology of the composite was completely different from those of GO and PPy.

The thermal stability of the GO film, pure PPy and the PPy/GR composite are shown in Figure 2, with the respective data summarized in Table I. The mass loss for all the samples at 100°C was due to the removal of absorbed water. Thermal decomposition of the GO sheets occurred in two steps, at 150 and 200°C. The weight loss at 150°C was due to the removal of labile oxygen functional groups, and the weight loss at 200°C was the result of GO reaching its deflagration point and the solid decomposing into carbon soot.[45] The weight of the PPy film remained around 90% at 250°C, and then gradually decreased

to 60% of the original at 650°C. The PPy/GR film showed a similar pattern of weight loss in the range of 250 to 650°C. However, additional weight loss occurred after 350°C, which could be caused by remnant oxygenous groups on graphene. The hybridization of GR and PPy was also supported by TGA analysis, where the profile of the composite lay between the profiles of GO and PPy. Moreover, the similarities in TGA profile between PPy and PPy/GR suggested uniform dispersion of GR in the PPy matrix.

Figure 3(a) shows wide scans of GO, PPy, and PPy/GR composite films, and Figure 3(b) exhibits the deconvoluted C_{1S} spectra of GO, PPy, and PPy/GR composite films. In Figure 3(a), the XPS wide scans of PPy and PPy/GR are similar to each another, indicating that the presence of graphene in PPy/GR was not influential enough to affect the peak intensities of the composite, due to the small concentration of GO used. The C_{1S} core level spectrum of the GO film could be fit into five component peaks with different binding energies. The peaks at 284.3 and 285.3 eV are attributed to sp^2 hybridized carbon and sp^3 hybridized carbon, respectively.[46] The peaks at 286.6, 287.0, and 288.6 eV are attributed to oxygenated carbons of C—O, C=O, and COOH, respectively.[47] The XPS spectrum of the pure PPy film
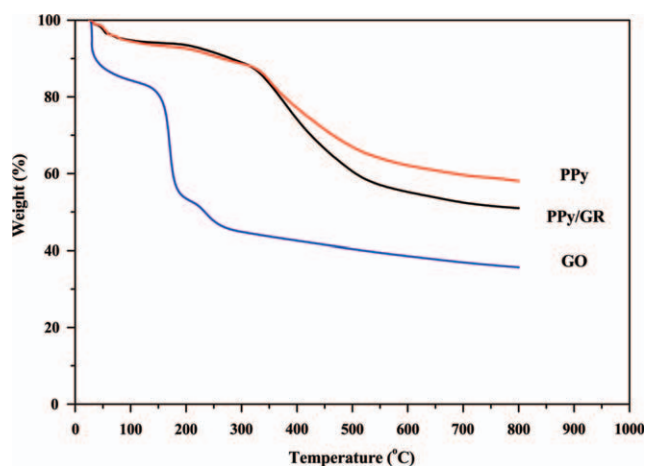

Figure 2. TGA of GO, PPy, and PPy/GR composite film, which represents all the composite films. The concentration of PPy used was 0.1*M*. [Color figure can be viewed in the online issue, which is available at wileyonlinelibrary.com.]

Table I. Thermogravimetric Analysis of GO, PPy, and PPy/GR Composite Film, Which Represents all the Composite Films

Sample	Weight %; 100°C	Weight %; 200°C	Weight %; 250°C	Weight %; 350°C	Weight %; 450°C	Weight %; 550°C	Weight %; 650°C
GO	84.32	53.48	47.67	43.62	41.46	39.44	37.73
PPy	94.53	92.62	90.71	84.22	71.52	64.02	60.79
PPy/GR	94.74	93.52	91.59	83.53	66.49	57.03	53.76

The concentration of PPy used was 0.1M.

demonstrated four component peaks, which were observed at 283.9, 284.4, 284.9, and 286.3 eV, suggesting the presence of sp^2 hybridized carbon, sp^3 hybridized carbon, C—N groups and the C—S group from NapTS as a dopant.[48] The XPS C_{1S} core level spectrum of the PPy/GR composite film could be fit into six component peaks with binding energies of 283.8, 284.5, 285.0, 286.2, 287.7, and 289.0 eV, which are attributed to sp^2 hybridized carbon, sp^3 hybridized carbon, C—N, C—O, C=O, and COOH.

The electrical conductivities of the composite films were determined by measuring their resistivities with a four-point probe. The average conductivities of composite films with various concentrations of pyrrole monomer are shown in Figure 4. The incorporation of 1 mg mL^{-1} of GO into the various concentrations of pyrrole greatly improved the conductivity of the composite films. For pure PPy, the magnitude of conductivity reached a maximum at a concentration of 0.2 mol dm^{-3} PPy, but decreased thereafter. However, in the case of PPy/GR composite films, the conductivities remained almost consistently high for concentrations of PPy above 0.1 mol dm^{-3}. Among all the samples, the PPy/GR composite film synthesized with 0.4 mol dm^{-3} pyrrole exhibited the highest conductivity (3862.87 S m^{-1}), which was two-fold higher than that of its pure counterpart (1806.49 S m^{-1}). The reported conductivity of PPy-graphene composites falls in the range of 102–793 S m^{-1}.[19,26,27,29,49] The low conductivity values of those composites were governed by the preparation method, surface functionalization of graphene, and the absence of a dopant. The current reported technique, comprising one-step electrodeposition in the presence of NapTS without the need to prereduce GO, shows great improvement on the conductivity of the composite films. As GO is known to be a nonconductive material, we are therefore convinced that the significant rise in conductivity of the composite films is contributed by the presence of graphene reduced from GO during the electrodeposition process. The increased conductivity of the composite films is also proof of the incorporation of graphene into the PPy polymer matrix (Figure 4).
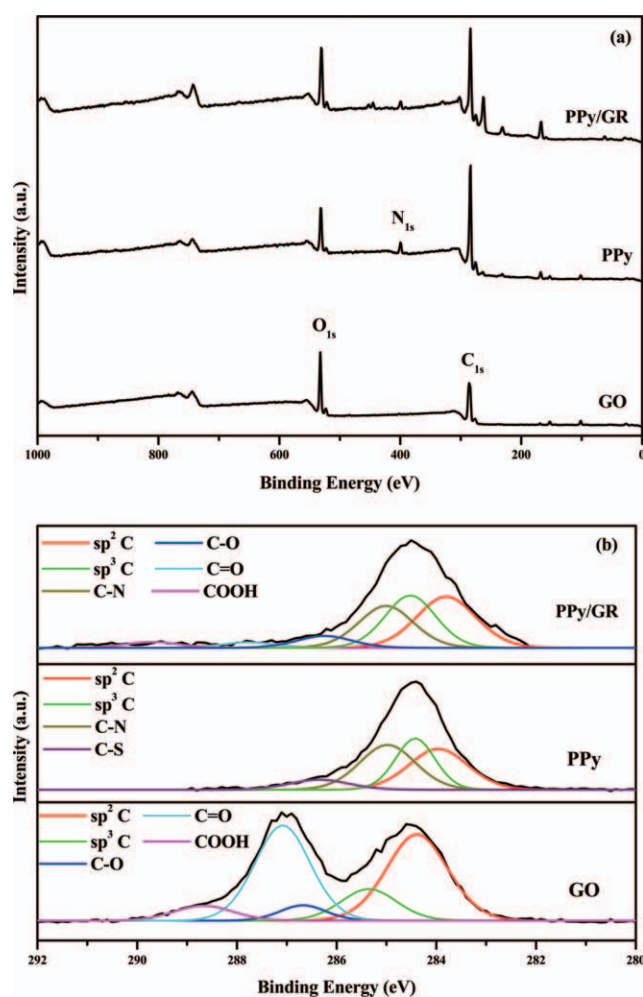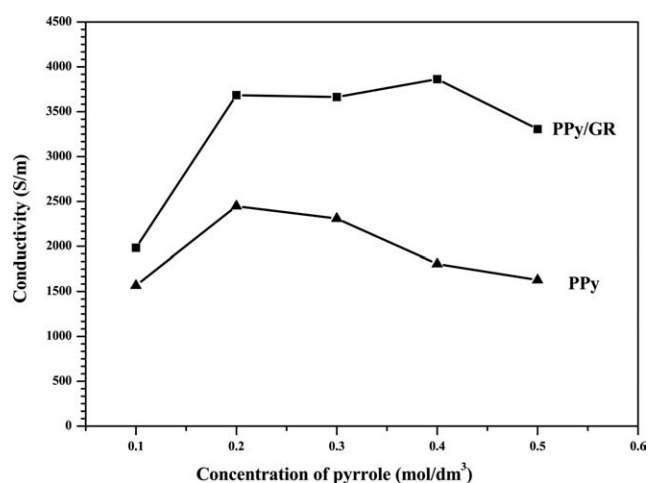

Figure 3. (a) Wide scans of GO, PPy, and PPy/GR composite film, and (b) deconvoluted XPS spectra of GO, PPy, and PPy/GR composite film, which represents all the composite films. The concentration of PPy used was 0.1M. [Color figure can be viewed in the online issue, which is available at wileyonlinelibrary.com.]

Figure 4. Conductivities of PPy and PPy/GR films.

Figure 5. Influence of GO concentration on the conductivities of PPy/GR composite films.
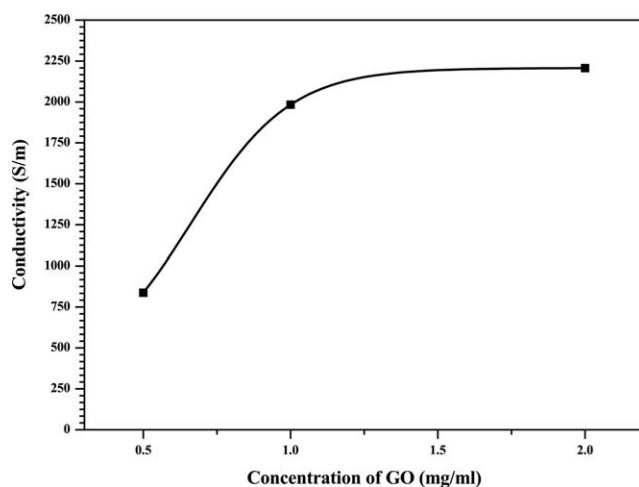

Figure 7. Influence of electrochemical deposition time on the conductivities of PPy/GR composite films.

The concentration of GO was varied between 0.5, 1, and 2 mg mL^{-1} to obtain the PPy/GR films, where [pyrrole] $= 0.1M$, [NapTS] $= 0.1M$ and the electrochemical deposition potential $= +0.8$ V/SCE. Figure 5 shows that increasing the GO concentration from 0.5 to 2 mg mL^{-1} led to an improvement in the PPy film's conductivity from 837.1 to 2206.4 S m^{-1}. A substantial increment of conductivity attributed to the increase in the GO concentration, as shown in Figure 5, was due to the formation of a conducting network by graphene in the polymer matrix, connecting the PPy conducting domains. The increase in conductivity is therefore due to a more conductive network within the composite system, hence increasing its electron mobility.[50]

Various electrochemical deposition potentials were applied to the aqueous electrolyte solution—+0.6 V/SCE, +0.8 V/SCE, +1.0 V/SCE, +1.3V/SCE, and +1.7V/SCE. Other polymerization parameters were kept constant at [pyrrole] $= 0.1M$, [NapTS] $= 0.1M$, and [GR] $= 1$ mg mL^{-1}. Figure 6 shows the dependence of the electrical conductivity of PPy/GR composite
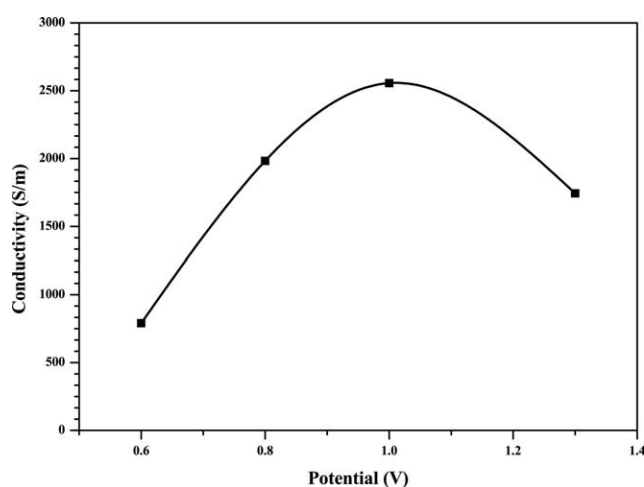

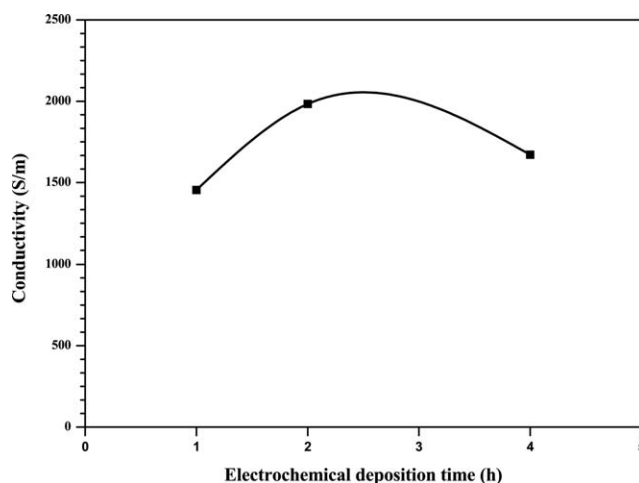**Figure 6.** Influence of electrochemical deposition potential on the conductivities of PPy/GR composite films.

films on the applied potential. The conductivities of PPy/GR composite films increased with increasing electrochemical deposition potential until +1.0 V/SCE, and decreased thereafter. Figure 6 suggests that the conductivity of the film is not only dependent on the concentration of pyrrole and graphene, but also on the applied potential. It has been reported that the poor conductivity of films prepared at low electrochemical deposition potentials results in shortened conjugation length, because oxygenation of active sites on the pyrrole ring is preferred compared to the polymerization reaction, leading to chain termination. On the other hand, over-oxidation may induce undesirable side reactions such as ring opening or breaking of the conjugated system, which leads to an enhancement of defects and results in films of lower conductivity.[51] This will also result in the addition of carbonyl and carboxylic groups to the polymer chains, which reduce the conductivity of the film.[52] At the applied voltage of +1.7 V/SCE, the over-oxidized film was fragile and brittle. The film tore to pieces during the peeling step; hence we were unable to measure its conductivity.

Aqueous electrolyte solutions were electrochemically polymerized at different deposition times of 1, 2, and 4 h, where [pyrrole] $= 0.1M$, [NapTS] $= 0.1M$, [GO] $= 1$ mg mL^{-1}, and +0.8 V/SCE were kept constant. Figure 7 shows that by increasing the deposition time from 1 to 2 h, the composite film's conductivity increased from 1454.5 to 1983.2 S m^{-1}. However, the conductivity dropped to 1671.4 S m^{-1} with an extended polymerization time. The increase in conductivity from 1 to 2 h of deposition time might be due to elongation of the conjugated chain length. However, extended deposition times will lead to excessive solvent uptake and hence, decrease the compactness of the PPy deposited in the composite. This will, in turn, create electrical isolation of PPy areas that will lead to a decrease in the conductivity of the composite film.[44]

CONCLUSION

In the present study, PPy/GR composite films were successfully synthesized by electrochemical deposition. This method offers a one-step synthesis of graphene-based composite films without

prereducing GO to graphene prior to incorporation into the host polymer. The conductivity of the PPy/GR composite films could be tuned by the concentration of PPy, the concentration of GO, the electrodeposition potential, and the reaction time.

REFERENCES

1. Skotheim, T. A.; Reynolds, J. R. Handbook of Conducting Polymers; CRC, New York, **2007.**

2. Boinowitz, T.; tom Suden, G.; Tormin, U.; Krohn, H.; Beck, F. *J. Power Sources* **1995,** *56*, 179.

3. Sun, W.; Zheng, R.; Chen, X. *J. Power Sources* **2010,** *195*, 7120.

4. Larmat, F.; Reynolds, J. R.; Qiu, Y. *Synth. Met.* **1996,** *79*, 229.

5. Jang, J.; Bae, J. *Sensors Actuat. B Chem.* **2007,** *122*, 7.

6. Lehr, I. L.; Saidman, S. B. *Electrochim. Acta* **2006,** *51*, 3249.

7. Yang, C.; Liu, P. *Synth. Met.* **2010,** *160*, 768.

8. Kanwal, F.; Siddiqi, S. A.; Batool, A.; Imran, M.; Mushtaq, W.; Jamil, T. *Synth. Met.* **2011,** *161*, 335.

9. Yalcinkaya, S.; Demetgul, C.; Timur, M.; Colak, N. *Carbohydr. Polym.* **2010,** *79*, 908.

10. Batool, A.; Kanwal, F.; Imran, M.; Jamil, T.; Siddiqi, S. A. *Synth. Met.* **2012,** *161*, 2753.

11. Chougule, M. A.; Sen, S.; Patil, V. B. *J. Appl. Polym. Sci.* **2012,** *125*, E541.

12. Yuan, Y.; Zhou, S.; Zhuang, L. *J. Power Sources* **2010,** *195*, 3490.

13. Lee, H.; Kim, H.; Cho, M. S.; Choi, J.; Lee, Y. *Electrochim. Acta* **2011,** *56*, 7460.

14. Singh, K.; Singh, B. P.; Chauhan, R.; Basu, T. *J. Appl. Polym. Sci.* **2012,** *125*, E235.

15. Konwer, S.; Maiti, J.; Dolui, S. K. *Mater. Chem. Phys.* **2011,** *128*, 283.

16. Jeevananda, T.; Kim, N. H.; Lee, J. H.; Basavarajaiah, S.; Deepa Urs, M.; Ranganathaiah, C. *Polym. Int.* **2009,** *58*, 775.

17. Liu, N.; Luo, F.; Wu, H.; Liu, Y.; Zhang, C.; Chen, J. *Adv. Funct. Mater.* **2008,** *18*, 1518.

18. Pumera, M. *Chem. Rec.* **2009,** *9*, 211.

19. Bose, S.; Kuila, T.; Uddin, M. E.; Kim, N. H.; Lau, A. K. T.; Lee, J. H. *Polymer* **2010,** *51*, 5921.

20. Dreyer, D. R.; Park, S.; Bielawski, C. W.; Ruoff, R. S. *Chem. Soc. Rev.* **2010,** *39*, 228.

21. Brownson, D. A. C.; Banks, C. E. *Analyst* **2010,** *135*, 2768.

22. Pan, D.; Wang, S.; Zhao, B.; Wu, M.; Zhang, H.; Wang, Y.; Jiao, Z. *Chem. Mater.* **2009,** *21*, 3136.

23. Liu, X.; Robinson, J. T.; Wei, Z.; Sheehan, P. E.; Houston, B. H.; Snow, E. S. *Diam. Relat. Mater.* **2010,** *19*, 875.

24. Brownson, D. A. C.; Kampouris, D. K.; Banks, C. E. *J. Power Sources* **2011,** *196*, 4873.

25. Han, Y.; Hao, L.; Zhang, X. *Synth Met* **2010,** *160*, 2336.

26. Bose, S.; Kim, N. H.; Kuila, T.; Lau, K.; Joong, H. L. *Nanotechnology* **2011,** *22*, 369502.

27. Zhang, D.; Zhang, X.; Chen, Y.; Yu, P.; Wang, C.; Ma, Y. *J. Power Sources* **2011,** *196*, 5990.

28. Nakui, H.; Okitsu, K.; Maeda, Y.; Nishimura, R. J. *Hazard. Mater.* **2007,** *146*, 636.

29. Si, P.; Ding, S.; Lou, X.; Kim, D. *RSC Adv.* **2011,** *1*, 1271.

30. Amarnath, C. A.; Hong, C. E.; Kim, N. H.; Ku, B.; Kuila, T.; Lee, J. H. *Carbon* **2011,** *49*, 3497.

31. Tully, E.; Higson, S. P.; O'Kennedy, R. *Biosens. Bioelectron.* **2008,** *23*, 906.

32. Zhang, J.; Kong, L.; Wang, B.; Luo, Y.; Kang, L. *Synth. Met.* **2009,** *159*, 260.

33. Torres, S.; Neculqueo, G.; Martinez, F. *J. Chil. Chem. Soc.* **2007,** *52*, 1235.

34. Tsai, M.; Chen, P.; Do, J. *J. Power Sources* **2004,** *133*, 302.

35. Zhang, H.; Xu, L.; Yang, F.; Geng, L. *Carbon* **2010,** *48*, 688.

36. Wu, H.; Qiu, X.; Cao, W.; Lin, Y.; Cai, R.; Qian, S. *Carbon* **2007,** *45*, 2866.

37. Chen, Y.; Li, Y.; Wang, H.; Yang, M. *Carbon* **2007,** *45*, 357.

38. Wu, H.; Tong, R.; Qiu, X.; Yang, H.; Lin, Y.; Cai, R.; Qian, S. *Carbon* **2007,** *45*, 152.

39. Yan, S.; Gao, Z.; Fang, Y.; Cheng, Y.; Zhou, H.; Wang, H. *Dyes Pigments* **2007,** *74*, 572.

40. Yang, Y.; Wang, C.; Yue, B.; Gambhir, S.; Too, C. O.; Wallace, G. G. *Adv. Energy Mater.* **2012,** *2*, 266.

41. Kupila, E.; Kankare, J. *Synth. Met.* **1993,** *55*, 1402.

42. Huang, N. M.; Lim, H. N.; Chia, C. H.; Yarmo, M. A.; Muhammad, M. R. *Int. J. Nanomed.* **2011,** *6*, 3443.

43. Geometric Factors in Four Point Resistivity Measurement, Bulletin No. 472–13; Haldor Topsoe Semiconductor Division, 2nd ed.; Haldor Topsoe: Denmark, **1968.**

44. de la Plaza, M. A.; Izquierdo, M. C. *Eur. Polym. J.* **2006,** *42*, 1446.

45. Kassaee, M. Z.; Motamedi, E.; Majdi, M. *Chem. Eng. J.* **2011,** *172*, 540.

46. Zhang, J.; Yu, Y.; Huang, D. *Solid State Sci.* **2010,** *12*, 1183.

47. Yumitori, S. *J. Mater. Sci.* **2000,** *35*, 139.

48. Ruangchuay, L.; Schwank, J.; Sirivat, A. *Appl. Surf. Sci.* **2002,** *199*, 128.

49. Liu, A.; Li, C.; Bai, H.; Shi, G. *J. Phys. Chem. C* **2010,** *114*, 22783.

50. Zengin, H.; Zhou, W.; Jin, J.; Czerw, R.; Smith, D. W.; Echegoyen, L.; Carroll, D. L.; Foulger, S. H.; Ballato, J. *Adv. Mater.* **2002,** *14*, 1480.

51. Satoh, M.; Kaneto, K.; Yoshino, K. *Synth. Met.* **1986,** *14*, 289.

52. Patois, T.; Lakard, B.; Martin, N.; Fievet, P. *Synth. Met.* **2010,** *160*, 2180.